Hayat Benassaoui[1], Said Abbout[1], El Hachmi Benassaoui[1], Mohamed Damej[1], Avni Berisha[2], Ahmed Dermaj[1], Meryem Zouarhi[3], Hicham Elmsellem[3], Driss Chebabe[1,4], Najat Hajjaji[1]*

[1]Team of Materials, Electrochemistry and Environment (LCOCE), Department of Chemistry, Faculty of Sciences, IbnTofail University, BP 133, 14000, Kenitra, Morocco, [2]Department of Chemistry, Faculty of Naturel and Mathematics Science, Prishtina University, Prishtina, Kosovo, Serbia, [3]The Higher Institute of Nursing Professions and Health Techniques (ISPITS) in Oujda, Morocco, [4]Laboratory of Materials Engineering for the Environment and Natural Resources, Faculty of Sciences and Techniques, University Moulay Ismail of Meknes, BP 509 Boutalamine 52000 Errachidia, Morocco

Scientificpaper
ISSN 0351-9465, E-ISSN 2466-2585
https://doi.org/10.62638/ZasMat1562

Zastita Materijala 67 ()
(2026)

Valorization of 1, 12-bis (4-amino-3-methyl-1, 2, 4-triazole)-5-S-dodecane on the corrosion of Bronze in 3.5% NaCl solution

ABSTRACT

The present study aimed to investigate the effect of a new triazole derivative, 1,12-bis(4-amino-3-methyl-1,2,4-triazole)-5-S-dodecane (dTC12)wassynthesized and characterized by NMR spectroscopy. The inhibition of dTC12 corrosion for Bronze in 3.5% NaCl solution was performed using potentiodynamic polarization and electrochemical impedance spectroscopy. The experimental results showthat the inhibitor effectively reduces the bronze B66 corrosion ratewhen themetal is directly immersed in the 3.5% NaCl solution containing dissolved inhibitor molecules. Polarization data indicates that the examined dTC12 acts as a mixedtype of inhibitor. The inhibit efficiency increases with increasing inhibitor concentration and immersion time in an aggressive medium. EIS results show that the change in impedance parameters with the concentration of inhibitor studied is indicative that the dTC12 acts by forming a thick film on the metal surface. This study is accomplished by in-depth theoretical calculations exploitation strategies supporting density functional theory (DFT/B3LYP) and molecular dynamics (MD) simulations.

Keywords: *Bronze B66, Corrosion, Inhibition, dTC12, Density Functional Theory, Molecular Dynamics*

1. INTRODUCTION

Bronze, a copper-based alloy, is widely used in marine engineering, architectural structures, industrial equipment, and cultural heritage artifacts due to its good mechanical strength, electrical conductivity, and relatively high corrosion resistance. However, when exposed to aggressive environments, particularly chloride-containing media such as seawater or saline atmospheres, bronze alloys can undergo significant corrosion degradation. Chloride ions can penetrate the naturally formed oxide layer on the alloy surface and accelerate electrochemical reactions responsible for metal dissolution and patina formation. The formation and characterization of corrosion products on bronze surfaces have been widely investigated because they directly influence the durability of bronze materials and the preservation of archaeological metallic artifacts [1,2].

Several protection strategies have been proposed to mitigate corrosion of copper and its alloys, including protective coatings, cathodic protection, and the use of corrosion inhibitors. Among these approaches, organic corrosion inhibitors represent one of the most practical and efficient methods due to their ease of application, relatively low cost, and high inhibition performance [3,4]. Organic inhibitors generally contain heteroatoms such as nitrogen, oxygen, or sulfur as well as aromatic rings or conjugated π-electron systems that facilitate adsorption on the metal surface and the formation of a protective barrier against corrosion [5].

Various classes of organic compounds have been investigated as corrosion inhibitors for copper and its alloys, including amines, imidazoles, pyridines, thiols, and azole derivatives [5,6]. Among them, azole-based compounds have been widely reported as highly effective corrosion inhibitors because of their ability to coordinate with copper atoms and form stable adsorption layers on the metal surface [6]. In particular, triazole derivatives have attracted considerable attention due to the presence of several nitrogen atoms within the

*Corresponding author: Meryem. Zouarhi
E-mail: meryem.zouarhi@uit.ac.ma
Paper received: 14. 09. 2025.
Paper corrected: 19.03.2026.
Paper accepted: 20.03.2026.

heterocyclic ring, which enhances their adsorption capability and interaction with metallic surfaces [7].

Several studies have demonstrated the effectiveness of triazole derivatives in inhibiting corrosion of copper and bronze alloys in chloride media. For example, Rahmouni et al. reported the significant inhibition performance of 3-methyl-1,2,4-triazole-5-thione for copper corrosion in NaCl solution containing sulphide ions [8]. Similarly, Chebabe et al. investigated the corrosion inhibition of bronze B66 in NaCl solution using 4-amino-3-methyl-1,2,4-triazole-5-thione, showing that the inhibitor effectively reduces the corrosion rate due to its adsorption on the metal surface [9]. Comparative studies performed by Benassaoui et al. further confirmed the efficiency of triazole derivatives for the protection of bronze alloys in chloride environments [10].

Other aminotriazole derivatives have also been reported as efficient inhibitors for copper alloys in saline media, showing strong adsorption properties and improved electrochemical behavior [11]. Recent studies have also highlighted the effectiveness of triazole derivatives as corrosion inhibitors for copper in chloride solutions through combined experimental and theoretical approaches such as density functional theory (DFT) and molecular dynamics simulations [12–15].

Despite the extensive research on triazole compounds, the development of new derivatives with improved inhibition efficiency remains an important research objective. In particular, molecules containing multiple heteroatoms and extended molecular structures may enhance adsorption strength and surface coverage, leading to improved corrosion protection. However, limited studies have investigated triazole derivatives containing long-chain sulfur-linked structures and multiple triazole functional groups for the corrosion protection of bronze alloys in chloride environments.

Therefore, the objective of the present work is to investigate the corrosion inhibition performance of a newly synthesized heterocyclic compound, 1,12-bis(4-amino-3-methyl-1,2,4-triazole)-5-S-dodecane (dTC12), for bronze B66 in near-neutral 3.5% NaCl solution. The inhibitor was synthesized, purified, and characterized using ^{1}H and ^{13}C NMR spectroscopy. The corrosion behavior of bronze in the absence and presence of the inhibitor was evaluated using potentiodynamic polarization and electrochemical impedance spectroscopy (EIS).

The obtained results show that the inhibition efficiency increases with inhibitor concentration and immersion time, reaching approximately 90% at 10^{-3} M, indicating the formation of a protective adsorbed film on the metal surface. In addition, theoretical calculations based on density functional theory (DFT) and molecular dynamics (MD) simulations were carried out to better understand the electronic properties and adsorption mechanism of the inhibitor molecules on the bronze surface.

2. EXPERIMENTAL

2.1. Material

The material used as the working electrode is bronze B66, its composition is given in Table1.

Table.1. Chemical composition of bronze B66 [16]

Element	Sn	Pb	Ni	Zn	Cu
Phase I (Wt %)	5.12	0.59	0.39	0.79	93.11
Phase II (Wt %)	21.29	1.69	0.38	0.29	76.35

2.2. Electrolytic medium

The aggressive solution (3,5% NaCl) was prepared by dilution of 35 g of NaCl with distilled water. This medium was used to increase the corrosive action of the solution.

2.3.Inhibitor tested

The 1,12-bis(4-amino-3-methyl-1,2,4-triazole)-5-S-dodecane is prepared in our laboratory by the condensation of 4-amino-3-methyl-1,2,4-triazole-5-thione and dodecane bromide. The resultant product characterized and identified by ^{1}H NMR, ^{13}C NMR (Fig. 1) [17].

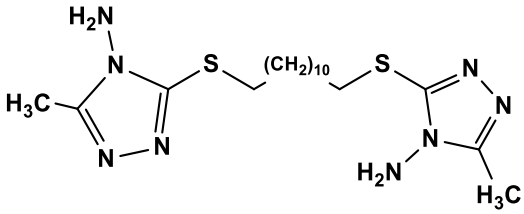

Figure 1. Molecular chemical structure of 1,12-bis(4-amino-3-methyl-1,2,4-triazole)-5-S-dodecane

This product was classified by ^{1}H NMR, ^{13}C NMR spectroscopy.

Spectral characteristics:

^{1}H NMR (300 MHz, DMSO):δ = 1.21-1.63 (m, 21H,$(CH_2)_{12}$); 2.25; 2.27 (d, 3H, CH_3), 3.042 (t, 2H, CH_2α), 5.7; 5.72 (d, 1 H, NH_2).

^{13}C NMR (75,47 MHz, DMSO):

- Alkyl chain:
  δ = 28.45; 28.92; 29.31; 29.56; 31.69.
- 1,2,4-triazole:

δ = 10.23 (CH_3), 151.17 (C_3, Har), 153.45 (C_5).

2.4. Electrochemical measurements

Electrochemical measurements were performed in a three-electrode cell. As the reference electrode was a saturated calomel electrode, the counter electrode was platinum, and the working electrode was used bronze electrode. The surface of contact with the corrosive solution is 0.78 cm². Before each test, the working electrode is polished using successive grits of emery paper (400; 600 and 1200), cleaned with acetone, washed with double-distilled water and finally dried with hot air.

The stationary measurements were carried out in potentiodynamic mode using a potentiometer / galvanostat SP-200 "biologic Science instruments". The working electrode is previously kept immersed at the free corrosion potential for one hour. The scanning speed is 1mV/s. The determination of the electrochemical parameters (icorr, Ecorr, βa and βc) from the polarization curves is done using a nonlinear regression by the original software 6.0. Thus, the inhibitory efficiency is calculated from the following formula:

$$E(\%) = \frac{I_{corr}^0 - I_{corr}}{I_{corr}^0} x\ 100$$

Where I_{corr}^0 and I_{corr} are the corrosion current densities obtained respectively without and with inhibitor.

Electrochemical impedance diagrams were plotted using the same instrument with a signal amplitude (10 mV). The frequency range explored varies from 100 KHz to 10 MHz. The simulation of the interface by an equivalent electrical circuit using the Ec-Lab simulation program was carried out.

The inhibitory efficacy was evaluated using the following equation:

$$E(\%) = \frac{R_t(inh) - R_t}{R_t(inh)} x\ 100$$

Where $R_t$and R_t(inh) are the charge transfer resistance respectively without and with inhibitors.

2.5. Computational details

All quantum calculations were performed by DFT with Becke's three-parameter exchange functional along with the Lee-Yang-Parr nonlocal correlation functional (B3LYP) [18] with the 6-311G++(d,p) basis set as implemented in Gaussian 03.

For an N-electron system with total energy E, qualitative chemical concepts electronegativity (χ) and hardness(η) are defined as the following first-order and second-order derivatives [19].

$$\chi = -(E_{HOMO}+E_{LUMO})/2$$

$$\eta = E_{LUMO} - E_{HOMO}$$

$$\Delta N = \frac{\chi_{Cu} - \chi_{Inh}}{2(\eta_{Cu} + \eta_{Inh})}$$

$$\Delta E_G = E_{LUMO} - E_{HOMO}$$

From the values of the total electronic energy, the ionization potential (I) and electron affinity (A) and the number of transferred electrons (ΔN) of the inhibitors are calculated using the following equations.

$$I = -E_{HOMO}$$

$$A = -E_{LUMO}$$

$$\Delta E_{bd} = -\eta/4$$

The Forcite module from Accelrys Inc. simulates the adsorption behavior. The surface $Cu_{111}$was chosen to simulate the adsorption process. The simulation of the interaction was carried out in a simulation box (2.3 × 2.3 × 3.84 nm) with periodic boundary conditions. Cutoff distance was 1.25 nm. Six layers of copper atoms were used to ensure that the depth of the surface was greater than the non-bond cutoff used in calculation. COMPASS forcefield was chosen to optimize the structures of all components of the system. The molecular dynamics simulation was carried out under 298 K, NVT ensemble, with a time step of 1 fs and simulation time of 1000 ps.

3. RESULTS AND DISCUSSION

3.1. Electrochemical study

3.1.1. Current-Potential curves

The polarization curves obtained for bronze B66 in the presence of dTC12 after 1 h of immersion at Ecorr are presented in Fig. 2. The curves recorded in the presence of the inhibitor were compared with those obtained in its absence in order to elucidate the inhibition mechanism of dTC12.

In the absence of inhibitor, the cathodic branch exhibits a mixed kinetic control near the corrosion potential. At higher cathodic overpotentials (E< −0.65 V/ECS), a limiting current density is observed, corresponding to the diffusion-controlled reduction of dissolved oxygen according to the following reaction [20]:

$$2H_2O + O_2 + 4e^- \rightarrow 4OH^-$$

Previous studies have shown that the corrosion process of bronze B66 in aerated neutral media is governed by a mixed kinetic mechanism involving both charge transfer and diffusion processes [21].

In the presence of dTC12, a significant decrease in current density is observed over the entire potential range. This reduction is attributed to the adsorption of inhibitor molecules on the bronze surface through their heteroatoms and π-electron systems, leading to the formation of a protective film that blocks active corrosion sites [22].

The cathodic reaction remains mainly controlled by oxygen reduction, which is the dominant process in aerated chloride media [13–15]. At more negative potentials, a slight increase in current density is observed, which can be attributed to the onset of hydrogen evolution (water reduction), although its contribution remains limited [8,22].

In the anodic domain, the polarization curves obtained in the presence of dTC12 are similar to those recorded in the absence of inhibitor, indicating that the inhibitor does not significantly affect the anodic dissolution mechanism of bronze. However, a slight decrease in anodic current density is observed for all concentrations, suggesting partial surface coverage and a weak blocking effect on anodic active sites [23].

A small shift of the corrosion potential (Ecorr) toward more positive values is observed in the presence of dTC12. However, this shift remains limited, and the more pronounced changes observed in the cathodic branch indicate that the inhibition mechanism is predominantly controlled by cathodic processes. Therefore, dTC12 can be classified as a predominantly cathodic-type inhibitor in chloride media [9,11,12].

Overall, the inhibition effect of dTC12 is mainly attributed to its adsorption on the metal surface, which reduces the number of active sites available for oxygen reduction and consequently decreases the overall corrosion rate. This behavior is consistent with previous studies on triazole-based inhibitors, where adsorption and protective film formation govern the inhibition performance [2,11,12].

The electrochemical parameters drawn from these two curves are shown in Table 2.

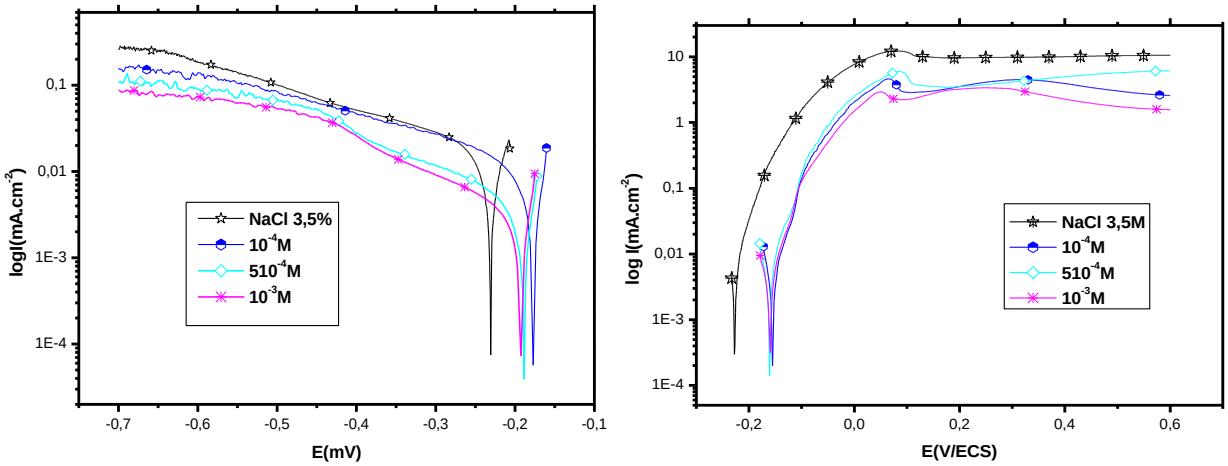

Figure 2. Effect of dTC12 concentration on the cathodic and anodic curves of bronze B66 in 3.5% NaCl

Table 2.Electrochemical parameters of B66 bronze polarization curves in 3.5% NaCl medium in the absence and presence of different concentrations of dTC12

		Cathodic domain			Anodic domain			IE (%)
		Ecorr (mV)	icorr (µA.cm-2)	bC (mV/dec)	Ecorr (mV)	icorr (µA.cm-2)	ba (mV/dec)	
3.5%NaCl	0	-233	7.85	-13.3	-230	7.85	39.2	---
Inhibitor (dTC12)	10^{-4}	-177	2.68	-18.3	-160	1.46	26	65.8
	5.10^{-4}	-160	1.24	-18.6	-177	1.32	28.5	84.5
	10^{-3}	-192	0.85	-35.5	-157	1.30	20.4	89.4

From the results obtained in Table 2, we conclude that:

- In the anodic domain, corrosion current densities (Icorr) decrease as the concentration in dTC12 increases. It is shifting the 7.85 µA.cm-2 in absence of an inhibitor [2] to 1.3 µA.cm-2 in the presence of 10^{-3}M of inhibitor.
- In the cathodic domain, the addition of dTC12 slightly changes the Ecorr values towards more cathodic values, and we note that the inhibitory efficacy E(%) hardly changes with increasing

inhibitor concentration. This result clearly indicates that dTC12 has no anodic effect. Therefore, it can be classified as a cathodic inhibitor in the marine environment.

3.1.2. Electrochemical impedance measurements

3.1.2.1. Effect of dTC12 Concentration

The study of the electrochemical behavior of B66 bronze corrosion in a 3.5% NaCl medium in the presence of dTC12 was also carried out by electrochemical impedance spectroscopy. The results obtained using this technique in a 3.5% NaCl medium containing different concentrations of inhibitor are shown in Nyquist diagrams (Fig.3).

From this figure, we observe that:

In the absence of an inhibitor, the impedance diagram observed after 60 minutes of immersion at the free corrosion potential of the B66 / NaCl interface indicates the presence of two capacitive loops.One at high frequencies related to the transfer of charge and one at low frequencies corresponds to surface heterogeneity.The model includes both charge transfer and faradic reactions above the surface, and it is widely reported in the literature for the investigation of copper alloys in NaCl aqueous solutions [23–25].

In the presence of an inhibitor, it is noted that the impedance diagrams registered are open semi-circles, lowly flat at high frequencies, showing a capacitive behavior of the sample in 3.5%NaCl.These diagrams show two capacitive loops with an increase in polarization resistance as a function of concentration.

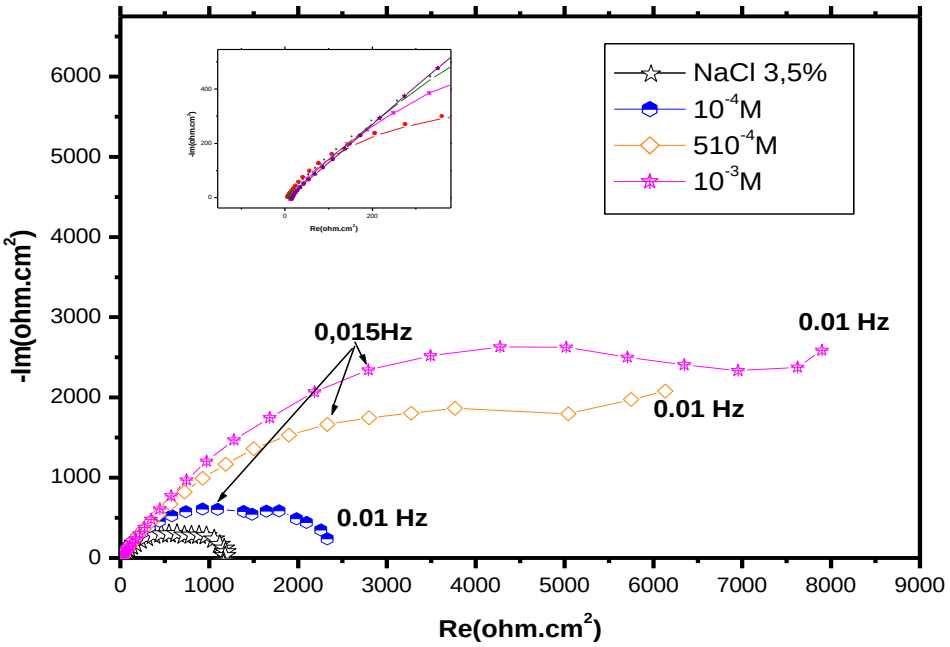

Figure 3. B66 bronze impedance spectra in 3.5% NaCl without and with addition of dTC12 for different concentrations of dTC12

The characteristic parameters associated to this impedance diagrams are given in Table 3.

Table.3. Electrochemical parameters of(Fig. 3)impedance diagrams.

dTC12	R_e (Ohm.cm²)	R_f (Ohm.cm²)	C_f (µF.cm^{-2})	R_t (Ohm.cm²)	C_t (µF.cm^{-2})	R_p (Ohm.m²)	IE%
0M	9,10	---	---	1190	264	3,86	---
10^{-4}M	9,23	6,21	12 ,78	926	142	1362,2	12
510^{-4}M	8,60	9,64	1,51	1021,6	58,31	6126	80
10^{-3}M	9,05	120,2	0,44	1317,7	10,52	12613	90

From Table 3, it can be noted that the Rp resistance increases with the inhibitor concentration, from 1190 Ω.cm^2 in the absence of an inhibitor [26] to 12613 Ω.cm^2 in the presence of 10^{-3} M in dTC12.The capacity associated with the high-frequency loop is very low so that it is allocated to the double layer for which the order of magnitude is generally a few tens of micro-farads, confirms the establishment of a relatively thick and compact film inhibitor on the metal surface [27].

The inhibition efficiency increases with the concentration of inhibitor; it reaches 90% for a concentration of 10^{-3} M in dTC12.

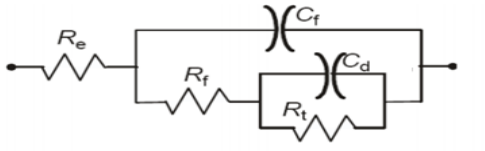

Figure 4. Electric equivalent circuit

These results are in good agreement with those found using stationary polarization curves. According to this observation, the following electrical equivalent circuit was proposed in (Fig.4).

3.1.2.2. Influence of immersion time

(Fig. 5) shows the electrochemical impedance diagrams of bronze in 3.5% NaCl medium, represented in the Nyquist plane, in the presence of 10^{-3}M of dTC12 for different immersion times.

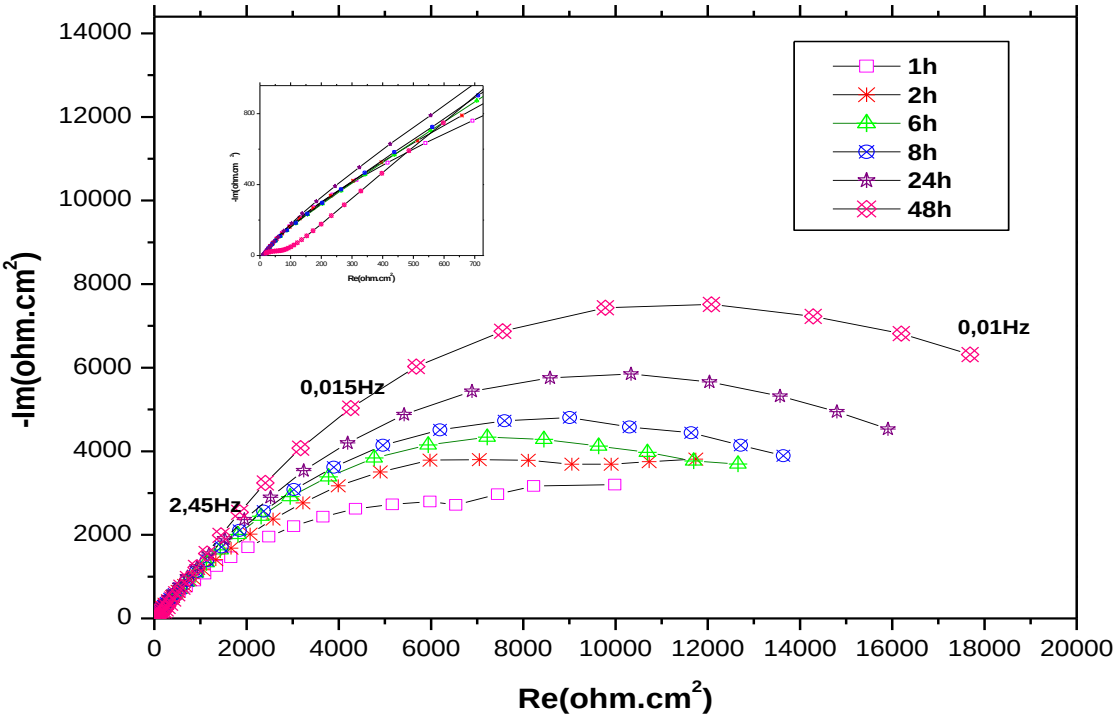

Figure 5. Niquist plots of the impedance data obtained from the bronze electrode exposed for different times to the 3.5% NaCl solution with 10^{-3} M dTC12

The Nyquist plots in (Fig.5)show that the diameter of the capacitive loopsincreases with immersion time, which implies that the bronze surface resistance improves with immersion time. The result is consistent with more corrosion products being deposited on the bronze surface and forming a relatively inert surface barrier at the bronze- solution interface.

3.2. Isotherm Adsorption

One of most method to determine the type of molecules adsorption is the Langmuir adsorption isotherm, which defined by the following equation [13],where the C_{inh} the inhibitor concentration and θ is thesurface coverage.

$$\frac{C_{inh}}{\theta} = \frac{1}{b} + C_{inh}$$

Plotting of the C_{inh}/θ versus the C_{inh} give a linear form, the result is given in the (Fig.6).

The linearization of the plot with R^2 equal to 0.99 suggest that the adsorption of the inhibitor molecules by forming a monolayer and no interaction between the inhibitor molecules. The standard adsorption energy calculated by using the below relation, where the R is the ideal gas constant, T is the temperature of the test equal to 298K and K is the inverse of the intercept the linear plot and the y axe [27-29].

$$\Delta G^{\circ}_{ads} = RTLn(55.5*K)$$

The Δ = -38.52 Kj/mol means the inhibitor molecules form a chemical and physical links with the electrode surface. This type of adsorption called mixed between physical and chemical adsorption.

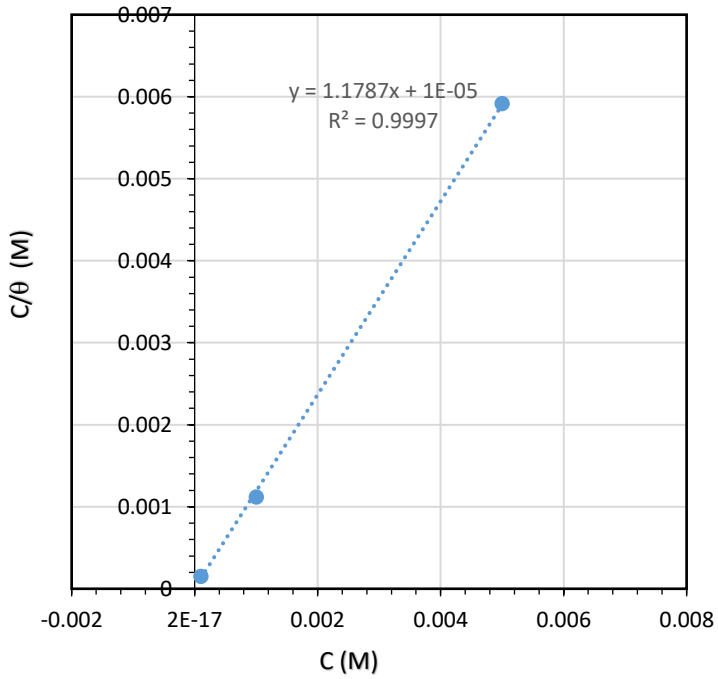

Figure 6. Langmuir plot of the bronze in the 3.5% NaCl solution

3.3. Quantum study

3.3.1. DFT Calculation

DFT is perf rmed to determine the HOMO and the LUMO distribution for the neutral and proton form. (Fig. 7)shows the result for this study. These results indicate that the electronic cloud of the proton IS biggest than the neutral form. Also, the donor-acceptor sites are localized around the heteroatoms (1,2,4-triazole ring)[30].

In addition, ESP maps for the two forms confirmed the HOMO and LUMO (Fig.8) observation because the electrophile and the nucleophile activate are located around the heteroatoms. While the red color indicates, the nucleophilic activity and blue indicate the electrophilic activity.

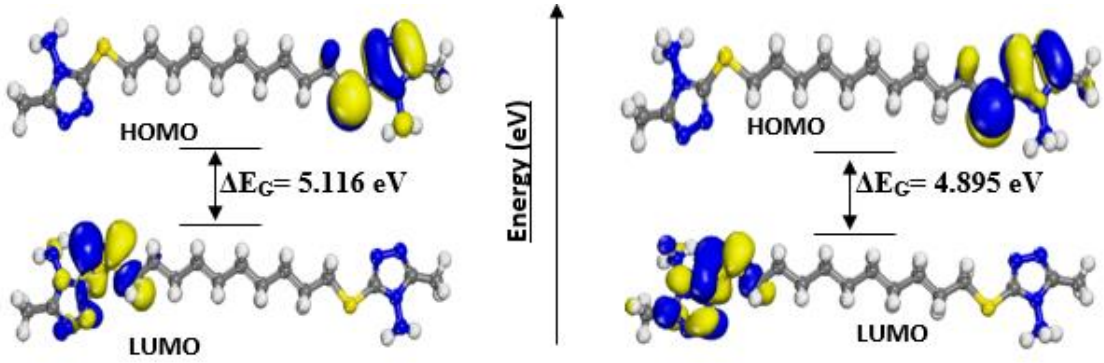

Figure 7. LUMO and HOMO orbitals of the neutral and protonforms of the dTC12 and the copper

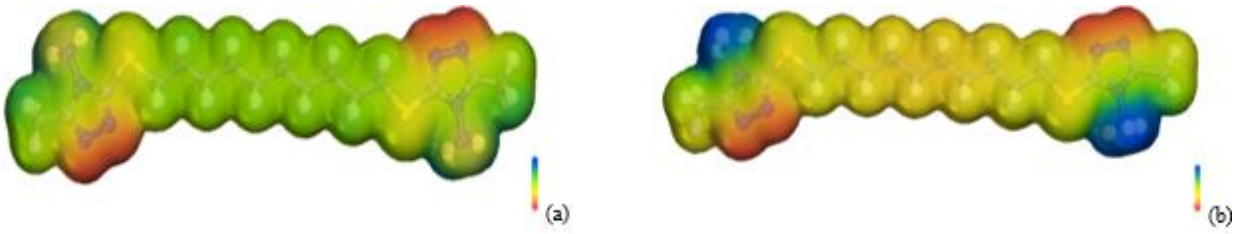

Figure 8. ESP distribution of the neutral (a) and proton (b) forms of the dTC12

The computed molecular properties, including E_{HOMO}, E_{LUMO}, $\Delta E_{LUMO-HOMO}$, dipole moment (μ), molecular volume (V), ionization potential (I), Electronegativity (χ),and fraction of transferred electrons (ΔN), are listed in table 4. As seen from the table, the positive ΔN value indicates that the electron transfer from the inhibitor molecule to the copper surface is available [31].

Table 4. DFT calculation parameters

Parameter	Neutral form	Proton form
E_{HOMO}	-5,726	-6,182
E_{LUMO}	-0,610	-1,287
Electronegativity (χ)	3,168	3,735
Gap energy (ΔE_G)	5,116	4,895
Hardness (η)	5,116	4,895
Fraction of electrons transferred (ΔN)	0,375	0,334
Back-donation (ΔE_{bd})	-1,279	-1,224

In frontier molecular orbital theory, the inhibition efficiency of the inhibitor is closely related to the HOMO and LUMO It is known that E_{HOMO} is often associated with the electron-donating ability of the inhibitor molecule, the higher values of E_{HOMO}, the greater ease of donating electrons to the unoccupied d orbital of metal. Whereas, E_{LUMO} indicates the ability of the molecule to accept electrons. So the lower the value of E_{LUMO}, the more probable that the molecule would accept electrons. Thus, higher E_{HOMO} and lower EL_{UMO} values generally enhance the inhibition efficiency. Moreover, the smaller value of $E_{LUMO}-E_{HOMO}$ energy gap (ΔE) for a protonated form, the higher the inhibition efficiency of that form. While the protonated form covers the good inhibition effect.

From table 4, the protoned form smeller value of the fraction of electrons transferred, Hardness and Back-donation, in addition, it has the biggest value of electronegativity. These results confirmed that the protonated form covers good inhibition efficiency.

3.3.2. Dynamic molecular

Molecular dynamics simulations were performed to study the adsorption behavior of specific inhibitor molecules onCu_{111} surface. The close contacts between the inhibitor molecules and copper surface as well as the best adsorption configurations for the compounds were depicted in (Fig.9).

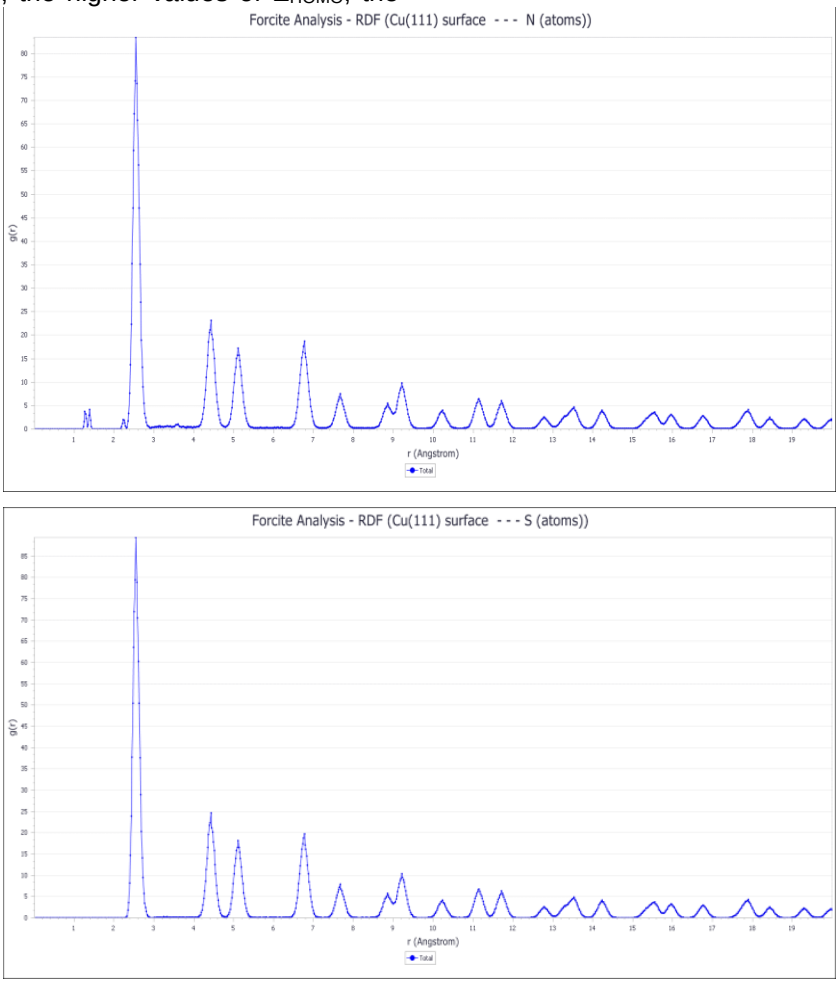

Figure 3. Paired correlation function of the dTC12/Cu_{111} surface

In addition, the adsorption behavior (i.e., chemical or physical adsorption) was evaluated from pair correlation function g(r) analysis using Forcite calculation code [27]. The intense peak(Fig. 9) occurred from 1Å up to 3.5Å, which is considered an indication of small bond length. This correlates to chemical adsorption, while physical adsorption is associated with an intense peak that is longer than 3.5Å [32].

It could be noticed that inhibitor adsorbed nearly parallel to the copper surface through donation of π electrons of the benzene rings and the lone pair of the heteroatoms to the metal. The average centroid distance (d) between inhibitors and the Cu_{111} surface is also shown in (Fig.10). The distance of dTC12 is short; this is due to triazole ring.

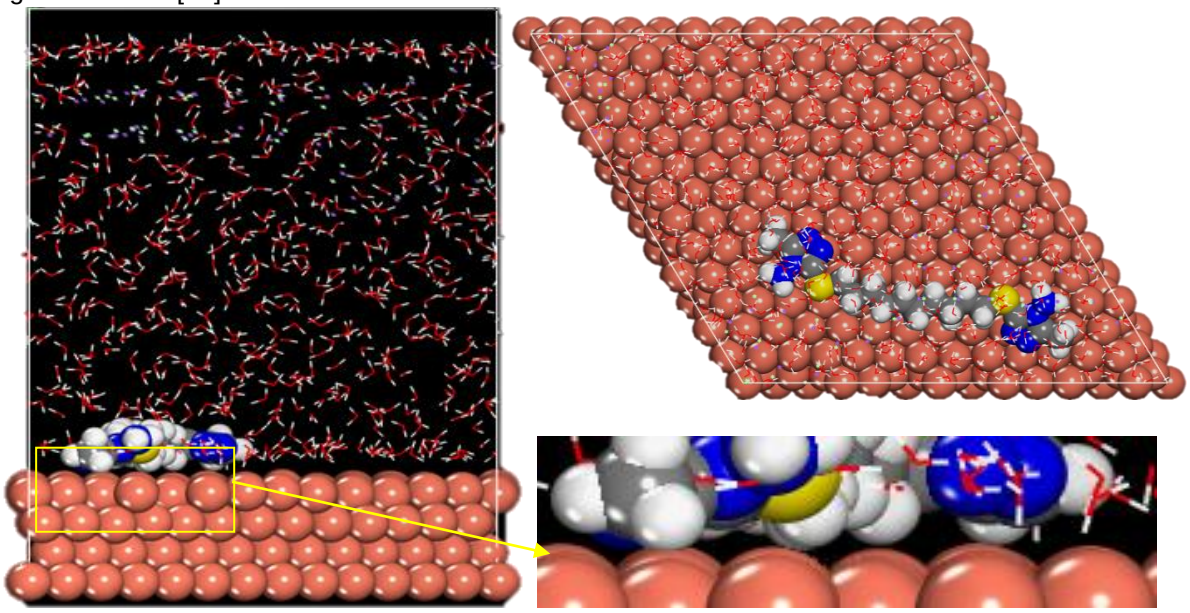

Figure 40. Top and side view

4. CONCLUSION

The 1,12-bis(4-amino-3-methyl-1,2,4-triazole)-5-S-dodecane (dTC12) molecule, was evaluated as corrosion inhibitors for B66 bronze corrosion in NaCl 3.5% using electrochemical methods, and computation calculations. In the study, the following conclusions were drawn:

- dTC12 displayed good protection efficiency for bronze corrosion in 3.5% NaCl and its performance increases with concentration and reinforced with immersion time.
- Polarization study suggested that dTC12 acted as cathodic-type inhibitor.
- EIS study suggested that dTC12 adsorb at interface using its electron-rich centers and acted as interface types of inhibitors. Its adsorption increased the values of polarization resistance.
- DFT study suggested that dTC12 interacted using donor-acceptor interactions in which electron-rich centers acted as sites for interactions.
- MD simulations showed that dTC12 strongly and spontaneously adsorbed over the metallic surface using flat or horizontal orientations.

Conflict of interest

The authors declare that they have no conflicts of interest.

5. REFERENCES

[1] G.Masi, J. Esvan, C. Josse, C. Chiavari, E. Bernardi, C. Martini, M.C. Bignozzi, N.Gartner, T. Kosec, L. Robbiola(2017) Characterization of typical patinas simulating bronze corrosion in outdoor conditions. Materials Chemistry and Physics, 200, 308–321. https://doi.org/10.1016/j.matchemphys.2017.07.091

[2] D.Chebabe, A.Dermaj, H.Erramli, N.Hajjaji (2014) Corrosion inhibition of bronze alloy B66 by 4-amino-3-methyl-1,2,4-triazole-5-thione in 3% NaCl solution. Anti-Corrosion Methods and Materials, 61(5), 281–286. https://doi.org/10.1108/ACMM-05-2013-1265

[3] H.Benassaoui, A.Dermaj, H.Erramli, M.Damej, N.Hajjaji, A.Srhiri(2015) Comparative corrosion inhibition study of bronze B66 alloy in 3.5% NaCl by 3-methyl-1,2,4-triazole-5-thione and 4-amino-3-methyl-1,2,4-triazole-5-thione. Organic Chemistry: An Indian Journal, 11(12), 433–441. https://www.tsijournals.com/abstract/comparative-corrosion-inhibition-study-of-bronze-b66-alloy-in-35-nacl-by-3methyl124triazole5thione-andrn4amino3methyl124-5210.html

[4] S.Abbout(2020) Green inhibitors to reduce the corrosion damage. In: Corrosion. Publisher: IntechOpen. License CC BY 3.0. https://doi.org/10.5772/intechopen.91481

[5] M.Zouarhi(2023) Bibliographical synthesis on the corrosion and protection of archaeological iron by green inhibitors. Electrochem, 4, 103–122. https://doi.org/10.3390/electrochem4010010

[6] M.Benmessaoud, M.SerghiniIdrissi, N.Labjar, K. Rhattas, M.Damej, N.Hajjaji, A.Srhiri, S.El Hajjaji (2016) Inhibition effect of aminotriazole derivative on the corrosion of Cu–40Zn alloy in 3% NaCl solution in presence of sulphide ions. Der Pharma Chemica, 8(4), 122–132. https://www.derpharmachemica.com/pharma-chemica/inhibition-effect-of-aminotriazole-derivative-on-the-corrosion-of-cu40zn-alloy-in-3nacl-solution-in-presence-of-sulphide.pdf

[7] N.Dang Nam, V.Quoc Thang, N.To Hoai, P.Van Hien (2016) Yttrium 3-(4-nitrophenyl)-2-propenoate used as inhibitor against copper alloy corrosion in 0.1 M NaCl solution. Corrosion Science, 112, 451–461.https://doi.org/10.1016/j.corsci.2016.08.005

[8] T.Yan, S.Zhang, L.Feng, Y.Qiang, L.Lu, D.Fu, Y.Wen, J.Chen, W.Li, B.Tan (2020) Investigation of imidazole derivatives as corrosion inhibitors of copper in sulfuric acid: Combination of experimental and theoretical researches. Journal of the Taiwan Institute of Chemical Engineers, 106, 118–129. https://doi.org/10.1016/j.jtice.2019.10.014

[9] Ž.Z.Tasić, M.B.Petrović Mihajlović, M.B.Radovanović, M.M.Antonijević(2019) New trends in corrosion protection of copper. Chemical Papers, 73, 2103–2132. https://doi.org/10.1007/s11696-019-00774-1

[10] S.Golfomitsou, J.F.Merkel (2004) Surface analysis of corroded silver coins from the wreck of the San Pedro De Alcantara (1786). In: Proceedings of Metal 2004, National Museum of Australia, Canberra, 344–368. https://www.nma.gov.au/_data/assets/pdf_file/0020/346043/NMA_metals_s2_p02_surface_analysis.pdf

[11] K.Rahmouni, N.Hajjaji, M.Keddam, A.Srhiri, H.Takenouti(2007)The inhibiting effect of 3-methyl-1,2,4-triazole-5-thione on corrosion of copper in 3% NaCl in presence of sulphide. Electrochimica Acta, 52, 7519–7526. https://doi.org/10.1016/j.electacta.2006.12.079

[12] M.Hrimla, A.Bouziani, A.Chahine, F.Aouini(2021) Overview on the performance of triazole derivatives as corrosion inhibitors for metals and alloys. Materials, 14, 7595. https://doi.org/10.3390/ma14247595

[13] M.Rbaa, B.Lakhrissi, M.Galai, M.E.Touhami, A.Zarrouk, I.Warad (2022) Triazole derivatives as efficient corrosion inhibitors for copper in chloride medium: Electrochemical and theoretical study. Journal of Molecular Liquids, 348, 118021. https://doi.org/10.1016/j.molliq.2021.118021

[14] M.Lasri, M.El Faydy, A.Zarrouk, R.Touir(2024) New triazole derivatives as corrosion inhibitors for copper in NaCl solution: Experimental and DFT study. Journal of Molecular Liquids, 390, 123201. https://doi.org/10.1016/j.molliq.2023.123201

[15] J.Liu, S.Zhang, W.Li, Y.Chen (2024) Corrosion inhibition performance of triazole derivatives for copper in chloride solutions: Experimental and theoretical insights. Applied Surface Science, 642, 158523. https://doi.org/10.1016/j.apsusc.2023.158523

[16] C.Degrigny, V.Argyropoulos, P.Pouli, M.Grech, K. Kreislova, M.Harith, F.Mirambet, N.Haddad, E. Angelini, E.Cano, N.Hajjaji, A.Ciringiroglu, A. Almansour, L.Mahfoud (2007) Proceedings of Metal 2007. Rijksmuseum, Amsterdam, p. 31.

[17] H.Benaassaoui(2018) Contribution to the protection of Bronze B66 against corrosion in 3.5% NaCl by new triazole derivatives. PhD Thesis (Chemistry), Kenitra, Morocco.

[18] A.D.Becke (1993) Density-Functional Thermo-chemistry. III. The Role of Exact Exchange. Journal of Chemical Physics, 98, 5648–5652. https://doi.org/10.1063/1.464913

[19] S.B.Liu (2009) Conceptual Density Functional Theory and Some Recent Developments. Acta Physico-Chimica Sinica, 25, 590–600. https://www.ingentaconnect.com/content/apcs/apcs/2009/00000025/00000003/art00033

[20] N.Saoudi, A.Bellaouchou, A.Guenbour, A.Ben Bachir, E.M.Essassi, M.El Achouri (2010) Aromatic quinoxaline as corrosion inhibitor for bronze in aqueous chloride solution. Bulletin of Materials Science, 33, 313–318. https://doi.org/10.1007/s12034-010-0048-2

[21] K.Rhattas, M.Benmessaoud, M.Doubi, N.Hajjaji, A.Srhiri(2011) Corrosion inhibition of copper in 3% NaCl solution by derivative of aminotriazole. Materials Sciences and Applications, 2, 220–225.https://www.scirp.org/html/4355.html

[22] S.Varvara, G.Caniglia, J.Izquierdo, R.Bostan, L.Gaina, O.Bobis, R.M.Souto (2020) Multiscale electrochemical analysis of corrosion control of bronze in simulated acid rain by horse-chestnut (Aesculus hippocastanum L.) extract as green inhibitor. Corrosion Science, 165, 108381. https://doi.org/10.1016/j.corsci.2019.108381

[23] K.Marušić, H.O.Ćurković, E.S.Lisac, H.Takenouti (2018) Two imidazole-based corrosion inhibitors for protection of bronze from urban atmospheres. Croatica Chemica Acta, 91(4), 435–446. https://doi.org/10.5562/cca3440

[24] K.Marušić, H.O.Ćurković, H.Takenouti(2011) Inhibiting effect of 4-methyl-1-p-tolylimidazole on corrosion of bronze patinated in sulphate medium. Electrochimica Acta, 56(22), 7491–7502. https://doi.org/10.1016/j.electacta.2011.06.107

[25] K.Marušić, H.O.Ćurković, H.Takenouti (2013) Corrosion inhibition of bronze and its patina exposed to acid rain. Journal of the Electrochemical Society, 160, C356–C363. https://iopscience.iop.org/article/10.1149/2.063308jes/meta

[26] K.Rahmouni, H.Takenouti, N.Hajjaji, A.Srhiri, L.Robbiola(2009)Protection of ancient and historic bronzes by triazole derivatives. Electrochimica Acta, 54(22), 5206–5215. https://doi.org/10.1016/j.electacta.2009.02.027

[27] S.Abbout, M.Zouarhi, D.Chebabe, M.Damej, A.Berisha, N.Hajjaji(2020) Galactomannan as a new bio-sourced corrosion inhibitor for iron in acidic media. Heliyon, 6(3), e03574. https://doi.org/10.1016/j.heliyon.2020.e03574

[28] S.Abbout, M.Chellouli, M.Zouarhi, B.Benzidia, D.Chebabe, A.Dermaj, H.Erramli, N.Bettach, N.Hajjaji(2018) New formulation based on Ceratonia siliqua L. seed oil as a green corrosion inhibitor of iron in acidic medium. Analytical and Bioanalytical Electrochemistry, 10(6), 789–804.

[29] H.Erramli, O.Dagdag, Z.Safi, N.Wazzan, L.Guo, S.Abbout, E.Ebenso, C.Verma, R.Haldhar, M.El Gouri (2020) Trifunctional epoxy resin as anticorrosive material for carbon steel in 1 M HCl: Experimental and computational studies. Surfaces and Interfaces, 21, 100707. https://doi.org/10.1016/j.surfin.2020.100707

[30] M.Serghini-Idrissi, M.C.Bernard, F.Z.Harrif, S.Joiret, K.Rahmouni, A.Srhiri, H.Takenouti, V.Vivier, M.Ziani (2005) Electrochemical and spectroscopic characterizations of patinas formed on an archaeological bronze coin. Electrochimica Acta, 50(24), 4699–4709. https://doi.org/10.1016/j.electacta.2005.01.050

[31] D.Chebabe, S.Abbout, M.Damej, A.Oubair, Z. Lakbaibi, A.Dermaj, H.Benassaoui, M.Doubi, N. Hajjaji (2020) Electrochemical and theoretical study of corrosion inhibition on carbon steel in 1 M HCl medium by 1,10-bis(4-amino-3-methyl-1,2,4-triazole-5-thioyl) decane. Journal of Failure Analysis and Prevention, 20, 1673–1683. https://doi.org/10.1007/s11668-020-00974-y

[32] H.Ma, S.Chen, L.Niu, S.Zhao, S.Li, D.Li(2002) Inhibition of copper corrosion by several Schiff bases in aerated halide solutions. Journal of Applied Electrochemistry, 32, 65–72. https://doi.org/10.1023/A:1014242112512

IZVOD

VALORIZACIJA 1,12-BIS(4-AMINO-3-METIL-1,2,4-TRIAZOL)-5-S-DODEKANA NA KOROZIJU BRONZE U 3,5% RASTVORU NaCl, EKSPERIMENTI I TEORIJSKA STUDIJA

Cilj ove studije bio je ispitivanje efekta novog derivata triazola, 1,12-bis(4-amino-3-metil-1,2,4-triazol)-5-S-dodekana (dTC12), koji je sintetisan i okarakterisan NMR spektroskopijom. Inhibicija korozije bronze izazvana dTC12 u 3,5% rastvoru NaCl izvršena je korišćenjem potenciodinamičke polarizacije i elektrohemijske impedansne spektroskopije. Eksperimentalni rezultati pokazuju da inhibitor efikasno smanjuje brzinu korozije bronze B66 kada je metal direktno uronjen u 3,5% rastvor NaCl koji sadrži rastvorene molekule inhibitora.

Podaci o polarizaciji ukazuju na to da ispitivani dTC12 deluje kao mešoviti tip inhibitora. Efikasnost inhibicije raste sa povećanjem koncentracije inhibitora i vremena uranjanja u agresivnu sredinu. Rezultati EIS-a pokazuju da promena parametara impedanse sa koncentracijom proučavanog inhibitora ukazuje na to da dTC12 deluje formiranjem debelog filma na površini metala.

Ova studija je postignuta detaljnim teorijskim proračunima i strategijama eksploatacije koje podržavaju teoriju funkcionala gustine (DFT/B3LYP) i simulacije molekularne dinamike (MD).

Ključne reči: Bronza B66, Korozija, Inhibicija, dTC12, Teorija funkcionala gustine, Molekularna dinamika

Naučni rad
Rad primljen: 14.09.2025.
Rad korigovan: 19.03.2026.
Rad prihvaćen: 20.03.2026.

Hayat. Benassaoui https://orcid.org/0000-0003-2532-7512
Said.Abbout https://orcid.org/0000-0001-8079-4979
Mohamed. Damej https://orcid.org/0000-0003-4917-3888
Avni. Berisha https://orcid.org/0000-0002-3876-1345
Ahmed. Dermaj https://orcid.org/0009-0002-9537-8809
Meryem. Zouarhi https://orcid.org/0000-0002-2123-0476
HichamElmsellem https://orcid.org/0000-0001-6882-9868
Driss. Chebabe https://orcid.org/0000-0002-1788-7942